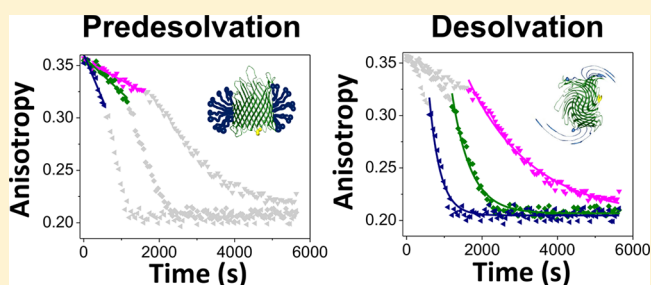


Kinetics of Membrane Protein–Detergent Interactions Depend on Protein Electrostatics

Aaron J. Wolfe,^{†,‡,⊥} Jack F. Gugel,^{†,⊥} Min Chen,[§] and Liviu Movileanu^{*,†,‡,||}[†]Department of Physics, Syracuse University, 201 Physics Building, Syracuse, New York 13244-1130, United States[‡]Structural Biology, Biochemistry, and Biophysics Program, Syracuse University, 111 College Place, Syracuse, New York 13244-4100, United States[§]Department of Chemistry, University of Massachusetts, 820 LGRT, 710 North Pleasant Street, Amherst, Massachusetts 01003-9336, United States^{||}Department of Biomedical and Chemical Engineering, Syracuse University, 223 Link Hall, Syracuse, New York 13244, United States

Supporting Information

ABSTRACT: Interactions of a membrane protein with a detergent micelle represent a fundamental process with practical implications in structural and chemical biology. Quantitative assessment of the kinetics of protein–detergent complex (PDC) interactions has always been challenged by complicated behavior of both membrane proteins and solubilizing detergents in aqueous phase. Here, we show the kinetic reads of the desorption of maltoside-containing detergents from β -barrel membrane proteins. Using steady-state fluorescence polarization (FP) anisotropy measurements, we recorded real-time, specific signatures of the PDC interactions. The results of these measurements were used to infer the model-dependent rate constants of association and dissociation of the proteomicelles. Remarkably, the kinetics of the PDC interactions depend on the overall protein charge despite the nonionic nature of the detergent monomers. In the future, this approach might be employed for high-throughput screening of kinetic fingerprints of different membrane proteins stabilized in micelles that contain mixtures of various detergents.



INTRODUCTION

Understanding the specific interactions at the protein–detergent complex (PDC) interface has critical importance to membrane protein structure,^{1,2} function,^{3,4} stability,^{5,6} and dynamics.^{7,8} Current approaches for an assessment of the PDC kinetics have numerous limitations. Available techniques are not amenable to high-throughput settings, are too highly specialized for a widespread adoption, or require high amounts of membrane protein. Because both the detergents and membrane proteins exhibit complex phases in solution,^{9–11} these challenges add up to a list of various difficulties for inferring a comprehensive determination of the forces that govern the kinetics of the PDC formation and dissociation. In many instances, the presence of protein aggregates,^{10,12} which coexist with both micelles and proteomicelles in solution, produces a significant deterioration in the signal-to-noise ratio of prevailing spectroscopic and calorimetric methods. These shortcomings are primarily determined by the direct relationship between the recorded readout and effective concentration of the detergent-solubilized membrane protein in solution.¹³ In the absence of a robust membrane protein scaffold that features programmable functional and biophysical properties,

obtaining the kinetic fingerprints at the PDC interface remains challenging. This gap of fundamental knowledge, which profoundly impacts structural biology and protein biotechnology, restrains the progress in the extensive screening of newly synthesized nonconventional detergents^{14–16} for membrane protein research.

To address these intimidating barriers, we developed a scalable approach for determining the real-time kinetic reads of the PDC interactions. This method is based upon a widely accessible, single-fluorophore probe technique. The pivotal concept of this study is the specific and sensitive modulation in the steady-state fluorescence polarization (FP) anisotropy^{17–20} of a membrane protein by alterations in its interfacial interactions with solubilizing detergent monomers. Dissociation of a membrane protein from a detergent micelle is accompanied by a decreased emission in the plane parallel to the polarized light and an increased emission to the plane orthogonal to the polarized light.²¹ In this way, the PDC

Received: August 13, 2018

Revised: September 24, 2018

Published: September 25, 2018

dissociation is accompanied by a decrease in the FP anisotropy, so the opposite is true for the PDC formation. Thus, the time-dependent steady-state FP anisotropy is recorded and processed as a ratio between the numbers of detergent-free and detergent-solvated membrane proteins.

β -barrel proteins are versatile to remodeling in various ways.^{22,23} The targeted panel in this study included the outer membrane protein G (OmpG),²⁴ a medium-sized, 14-stranded β -barrel ($pI = 4.4$; Figure 1A), and three homologous variants

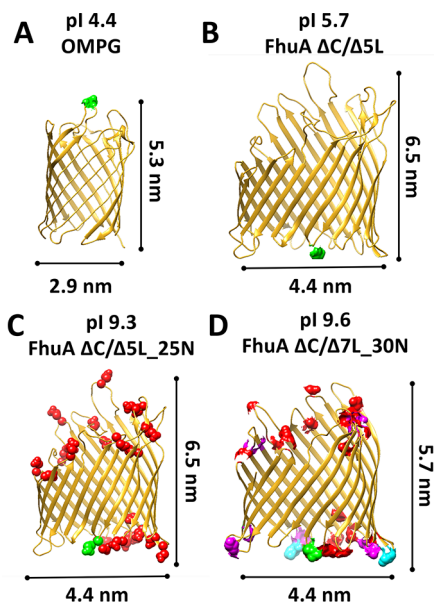


Figure 1. Structural homology models of the four proteins explored in this work. (A) OmpG, (B) FhuA $\Delta C/\Delta 5L$, (C) FhuA $\Delta C/\Delta 5L_{25N}$, and (D) FhuA $\Delta C/\Delta 7L_{30N}$. The native residues are shown in gold. Charge neutralizations that occur in both FhuA $\Delta C/\Delta 5L_{25N}$ and FhuA $\Delta C/\Delta 7L_{30N}$ are shown in red. Additional charge reversals⁵⁷ that occur only in FhuA $\Delta C/\Delta 7L_{30N}$ are shown in cyan. Other noncharge altering mutations of FhuA $\Delta C/\Delta 7L_{30N}$, with respect to FhuA $\Delta C/\Delta 5L_{25N}$, are shown in magenta. For each protein, the position of Texas Red³⁷ is labeled in green. The corresponding isoelectric point (pI) of each protein is presented on the top of individual panels.

of the ferric hydroxamate uptake component A (FhuA) of *E. coli*, a large 22-stranded β -barrel (Figure 1B–D).²⁵ The monomeric nature of these outer membrane proteins is advantageous for both the preparative steps^{26–28} and further data analysis of the steady-state FP anisotropy recordings.²¹ In order to explore the effect of the protein charge on the PDC kinetics, we conducted local and global protein engineering of FhuA. The 505-residue FhuA $\Delta C/\Delta 5L$ protein is an extensive truncation mutant of the wild-type, 714-residue FhuA, lacking an N-terminal, 160-residue cork domain and five large extracellular loops ($pI = 5.7$; Figure 1B).²⁹ Furthermore, dramatic alterations in the charge of the acidic FhuA $\Delta C/\Delta 5L$ protein were conducted by neutralizing its 25 and 30 negative charges, resulting in two basic β -barrels, FhuA $\Delta C/\Delta 5L_{25N}$ ($pI = 9.3$; Figure 1C) and FhuA $\Delta C/\Delta 7L_{30}$ ($pI = 9.6$; Figure 1D), respectively. In this way, the targeted panel in this work included two acidic and two basic proteins, out of which the 281-residue OmpG protein featured a relatively smaller size than that of the three homologous FhuA variants. This experimental design enabled us to observe whether a change in the membrane protein size has a significant impact on the

steady-state FP anisotropy. Notably, the truncation FhuA variants exhibit a fairly stable β -barrel scaffold under a very broad range of experimental conditions, including very acidic pH,^{30,31} highly osmotic^{26,32} or electro-osmotic pressure,³⁰ and elevated temperatures.³⁰ In addition, the stability of FhuA is not impaired by local and global modifications even when accommodating newly functional polypeptides within the pore interior.³¹

Very recently, we showed that the desorption of detergent monomers from membrane proteins undergoes two distinct phases: a slow detergent predesolvation, which is highlighted by a minor and linear decrease in the FP anisotropy (Figure 2A), and a fast detergent desolvation, which is characterized by a drastic, exponential-decay change in the FP anisotropy (Figure 2B).³³ In this work, we systematically examined the kinetic reads of the PDC interactions for β -barrel membrane proteins of varying surface charge. Specifically, we were able to probe time-dependent FP anisotropy changes at detergent concentrations comparable with and below the critical micelle concentration (CMC) but keeping the protein concentration constant at a low-nanomolar level. Our method enables model-dependent determinations of the kinetic rate constants and equilibrium dissociation constants of the proteomicelles. These interfacial PDC interactions were inferred for two nonionic, maltoside-containing detergents, whose CMC values are in the millimolar range. In the future, this method might be employed for rapid screening of the kinetic reads of proteomicelles under a broad range of physical and chemical conditions.

METHODS

Cloning, Expression, and Purification of Membrane Proteins. The *fhuA* $\Delta c/\Delta 5l$ gene, which lacked the regions coding for five extracellular loops L3, L4, L5, L10, and L11, as well as the cork domain (C), was produced through de novo synthesis (Geneart, Regensburg, Germany).^{27,31} The *fhuA* $\Delta c/\Delta 5l_{25n}$ and *fhuA* $\Delta c/\Delta 7l_{30n}$ genes were generated by Integrated DNA Technologies (IDT, Coralville, IA) in pIDTSmart Amp vector. All genes included a 3' thrombin site and 6 \times His⁺ tag. *fhuA* $\Delta c/\Delta 5l_{t7}$ was developed using inverse PCR and pPR-IBA1-*fhuA* $\Delta c/\Delta 5l$ -6 \times His⁺ as a template. The PCR product was self-ligated for the creation of pPR-IBA1-*fhuA* $\Delta c/\Delta 5l_{t7}$ -6 \times His⁺. The T7 β turn (V³³¹PEDRP³³⁶) was replaced with a cysteine-containing, GS-rich flexible loop (GGSSGCGSSGGS) for the fluorophore grafting. A similar approach was used for the mutagenesis within the *fhuA* $\Delta c/\Delta 5l_{25n}$ and *fhuA* $\Delta c/\Delta 7l_{30n}$ genes. Protein expression and extraction of truncation FhuA^{29,32} mutants and OmpG^{34,35} proteins were previously reported. In the case of OmpG, the cysteine sulfhydryl was engineered at position D224, on extracellular loop L6, using single-site mutagenesis PCR.

Refolding of Proteins. A rapid-dilution refolding protocol was used for the refolding of all proteins.³⁰ Then, 40 μ L of purified and guanidinium hydrochloride (Gdm-HCl)-denatured protein was 50-fold diluted into 200 mM NaCl, 50 mM HEPES, pH 7.4 solutions at 4 $^{\circ}$ C, which contained detergents (Anatrace, Maumee, OH) at concentrations above their CMC. Detergent solutions were freshly produced to avoid their oxidation and hydrolysis.³⁶ Different incubation detergent concentrations were prepared, as follows: (i) 5, 20, and 50 mM *n*-decyl- β -D-maltopyranoside (DM) and (ii) 50 mM 4-cyclohexyl-1-butyl- β -D-maltoside (CYMAL-4).

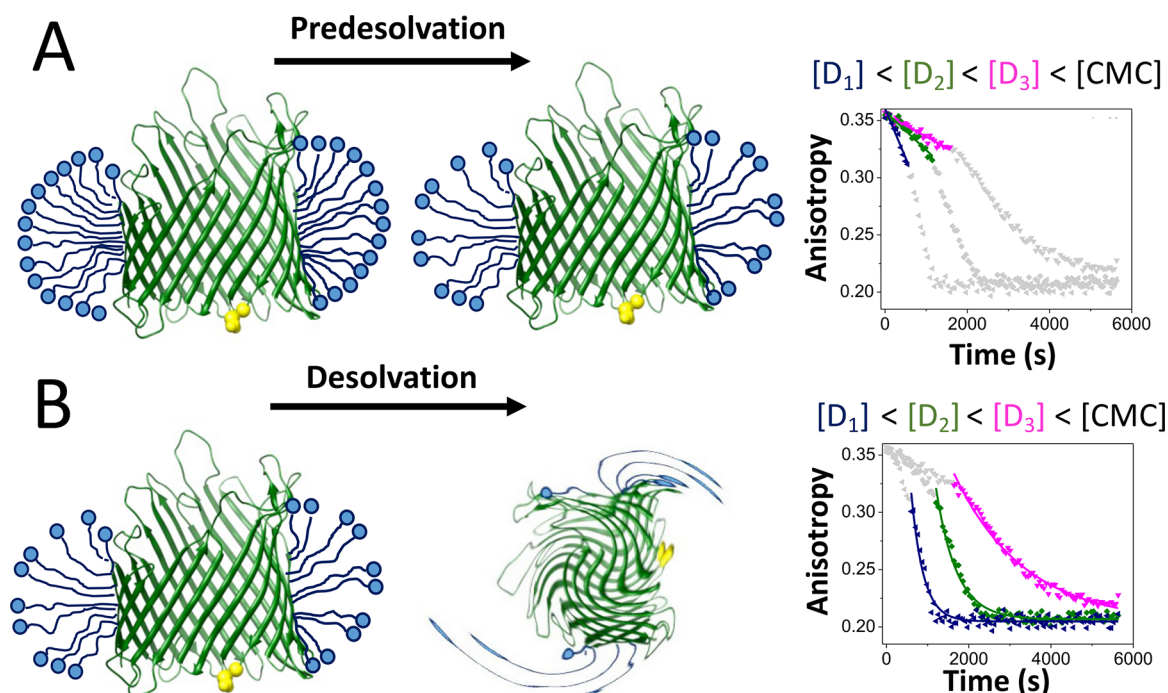


Figure 2. Cartoon illustrating the two phases noted as a result of detergent depletion within the sample well. (A) Predesolvation; (B) Detergent desolvation. Predesolvation phase is accompanied by the dissociation of a small number of detergent monomers from proteomicelles, contributing to a low modification of the FP anisotropy. Detergent desolvation is a rapid dissociation of numerous detergent monomers in single-exponential decay fashion. The right-hand panels show typical trajectories of the FP anisotropy of the predesolvation and desolvation phases for various detergent concentrations below the CMC.

Fluorescent Labeling of the FhuA and OmpG Proteins. Texas Red C2-maleimide (Thermo Fisher Scientific) was used for fluorescent labeling of all membrane proteins, as previously reported.²¹

Steady-State FP Anisotropy Recordings. Time-dependent FP anisotropy traces were acquired using a SpectraMax I3 plate reader (Molecular Devices, Sunnyvale, CA) equipped with a Paradigm detection cartridge for rhodamine FP spectroscopy.²¹ These measurements were conducted using 96-well Costar assay plates (Corning Incorporated, Kennebunk, ME). The wavelengths of excitation and emission were 535 and 595 nm, respectively. The attachment site of Texas Red was chosen on the water-soluble domains of the membrane proteins, because of the hydrophilic nature of this fluorophore.³⁷ The FP anisotropy depended on the orthogonal, $I_0(t)$, and parallel, $I_p(t)$, emission intensities:^{38,39}

$$r(t) = \frac{I_p(t) - GI_0(t)}{I_p(t) + 2GI_0(t)} \quad (1)$$

where G is a sensitivity correction factor for the detection modes when emission polarizers are oriented vertically and horizontally, as follows:

$$G = \frac{I_{HV}}{I_{HH}} \quad (2)$$

Here, I_{HH} is the intensity with both the excitation and emission polarizers in a horizontal orientation, whereas I_{HV} shows the intensity with the excitation and emission polarizers oriented horizontally and vertically, respectively. The experimental FP data were presented as average \pm SD over a number of at least three distinct acquisitions. The time-dependent, steady-state FP anisotropy traces were acquired with diluted detergents,

while keeping the final protein concentration constant at 28 nM. These detergent dilutions were conducted by titrating the refolded protein samples with buffer containing detergents at various concentrations. The final detergent concentration was inferred using the equation:

$$C_f V = C_s V_s + C_d V_d \quad (3)$$

V and C_f indicate the well volume and final detergent concentration of the protein sample, respectively. C_s and C_d show the detergent concentrations of the refolded protein (starting concentrations) and diluting buffer, respectively. V_s and V_d denote the volume of the refolded protein sample at a starting detergent concentration and the volume of the diluting buffer containing detergent at a given concentration, respectively. For DM, we used three concentrations below the CMC (0.45, 0.85, and 1 mM) and four concentrations above the CMC (2.5, 5, 10, and 20 mM). For CYMAL-4, four concentrations below the CMC (1, 2, 4, and 7 mM) and two concentrations above the CMC (12 and 50 mM) were employed. It was noted that in the case of DM-solvated FhuA variants the FP anisotropy curves were very noisy at extreme pH values (e.g., pH 4.6 and pH 10.0) and detergent concentrations lower than 1 mM. This outcome precluded the determination of statistically significant rate constants of association and dissociation. In addition, the FP anisotropy decayed even at detergent concentrations above the CMC, suggesting a slow increase in the tumbling rate of the proteomicelles under these experimental conditions. Therefore, we expanded the dilution spectrum of DM in the range of 1–50 mM for these specific cases. The self-quenching of Texas Red did not induce a time-dependent reduction in the FP anisotropy.³⁵ Radical detergent depletion within the wells increased protein aggregation, but without impacting the

optical signal-to-noise ratio of the FP anisotropy. The experimental uncertainty was affected at detergent concentrations below the CMC as compared to that at concentrations above the CMC, most likely because of the coexistence of complex substates produced by soluble and insoluble protein aggregates.

Minimizing the Effects of Light Scattering. These studies involved the presence of nanoscopic particles within the sample well, such as detergent micelles, proteomicelles, and protein aggregates. Therefore, these steady-state FP anisotropy recordings were subject to light scattering signals produced by these particles in solution and at detergent concentrations either below or above the CMC. The major contributions to light scattering are the Rayleigh and Raman factors, which are characterized by light intensity functions proportional to the power of λ^{-4} , where λ is the emission wavelength.^{20,40} For that reason, our assay was conducted using a long emission wavelength. Moreover, the concentration of the Texas Red-labeled proteins was increased up to a critical value, beyond which the FP anisotropy readout was independent of the protein concentration.³⁵ In addition, SpectraMax I3 plate reader features excitation and emission filters that form a spectral gap of 60 nm, contributing to a reduction in the light scattering signals. Finally, additional control experiments reinforced the minimized contributions of light scattering to the FP anisotropy readout. For example, at increased detergent concentrations above the CMC, the FP anisotropy readout reached a well-defined plateau with a maximum value, r_{\max} . In the presence of significant light scattering contributions, enhanced concentrations of detergent micelles above the CMC would gradually increase the steady-state FP anisotropy, which was not found in our studies.

Analysis of the Predesolvation and Desolvation Rates. The observed predesolvation rate constants ($k_{\text{obs}}^{\text{pre}}$) were determined using a linear fit of the time-dependent FP anisotropy, $r(t)$, at detergent concentrations below the CMC (Supporting Information, Tables S1–S8):

$$r(t) = -k_{\text{obs}}^{\text{pre}}t + r_{\max} \quad (4)$$

where r_{\max} is the maximum FP anisotropy recorded at time zero. Here, t is the recording time during the predesolvation phase. In fact, $k_{\text{obs}}^{\text{pre}}$ is the apparent zero-order rate constant for the predesolvation reaction of the proteomicelles. On the other hand, the observed desolvation rate constants, $k_{\text{obs}}^{\text{des}}$, were determined at various detergent concentrations below the CMC using a single-exponential fit of the time-dependent FP anisotropy (i.e., $k_{\text{obs}}^{\text{des}}$ is $1/\tau$, where τ is the desolvation time constant):

$$r(t) = r_{\text{d}}e^{-t/\tau} + r_{\min} \quad (5)$$

where r_{\min} is the minimum recorded FP anisotropy at time infinity of the desolvation phase. t indicates the recorded time during the desolvation phase. This time includes the total time of the predesolvation phase, T^{pre} . In general, the observed desolvation rate constant, $k_{\text{obs}}^{\text{des}}$, was determined by a single-exponential decay fit of the time-dependent FP anisotropy, $r(t)$. In fact, $k_{\text{obs}}^{\text{des}}$ is the apparent first-order rate constant⁴¹ for the desolvation reaction of the proteomicelles. This rate constant includes a composite mixture of the kinetic rate constants of association (k_{on}) and dissociation (k_{off} ; Supporting Information).⁴² Deviations from this pattern occurred in a number of cases that were treated by a linear time-dependence

fit. In eq 5, r_{d} is a constant, so that the initial FP anisotropy during the desolvation phase, r_{in} , is given by the following equation:

$$r_{\text{in}} = r(T^{\text{pre}}) = r_{\text{d}}e^{-T^{\text{pre}}/\tau} + r_{\min} \quad (6)$$

which provides the r_{d} constant:

$$r_{\text{d}} = \frac{r_{\text{in}} - r_{\min}}{e^{-T^{\text{pre}}/\tau}} \quad (7)$$

Using eqs 5 and 7, one derives the time-dependent FP anisotropy for the detergent desolvation phase of proteomicelles:

$$r(t) = (r_{\text{in}} - r_{\min})e^{-t-T^{\text{pre}}/\tau} + r_{\min} \quad (8)$$

The time-dependent protein concentration that is still detergent solvated, $[P(t)]$, is given by the following equation:

$$[P(t)] = [P_t] \left(\frac{r(t) - r_{\min}}{r_{\text{in}} - r_{\min}} \right) \quad (9)$$

Therefore, the time-dependent observed desolvation rate is

$$R^{\text{des}}(t) = \left| \frac{d[P(t)]}{dt} \right| = [P_t] \frac{1}{\tau e^{-t-T^{\text{pre}}/\tau}} \quad (10)$$

where $[P_t]$ is the total protein concentration at the beginning of the desolvation process. At the initial time of the desolvation process, $t = T^{\text{pre}}$. Consequently, the initial observed desolvation rate, $R_{\text{in}}^{\text{des}}$, is the following:

$$R_{\text{in}}^{\text{des}} = \frac{[P_t]}{\tau} = [P_t]k_{\text{obs}}^{\text{des}} \quad (11)$$

Here, $\Delta r = r_{\text{in}} - r_{\min}$ is the absolute FP anisotropy change during the desolvation phase. Finally, the time-independent rate of the protein predesolvation is the following:

$$R^{\text{pre}} = \frac{[P_t]}{T^{\text{pre}}} \quad (12)$$

RESULTS

Kinetics of the Neutral Detergent–Membrane Protein Interactions are pH Dependent. Prior steady-state FP anisotropy studies under equilibrium conditions demonstrated that the apparent dissociation constant, K_{d} , of proteomicelles with maltoside-containing detergents is not generally affected by the pH.³⁵ Here, we inspected whether this is also true for the kinetic reads of proteomicelles containing either *n*-decyl- β -D-maltopyranoside (DM) or 4-cyclohexyl-1-butyl- β -D-maltoside (CYMAL-4), two nonionic detergents. DM encompasses a medium-sized hydrophobic chain with 10 alkyl carbons. CYMAL-4 includes a short hydrophobic chain with four alkyl carbons and a cyclohexyl group. The CMC values of DM and CYMAL-4 are ~ 1.8 and 7.6 mM, respectively.^{21,36} We found that, at detergent concentrations much greater than the CMC, there was no significant alteration in the FP anisotropy (Figures 3–7; Supporting Information, Figures S1–S3).²¹ Under these conditions, both OmpG⁴³ and truncation FluA^{21,27} variants were fully detergent-solvated and showed a preponderant β -sheet structure in solution. Thus, the proteomicelles reached the slowest rotational mobility, which corresponded to the highest FP anisotropy value, r_{\max} . However, at detergent concentrations comparable with or below the CMC, the FP anisotropy showed drastic changes as

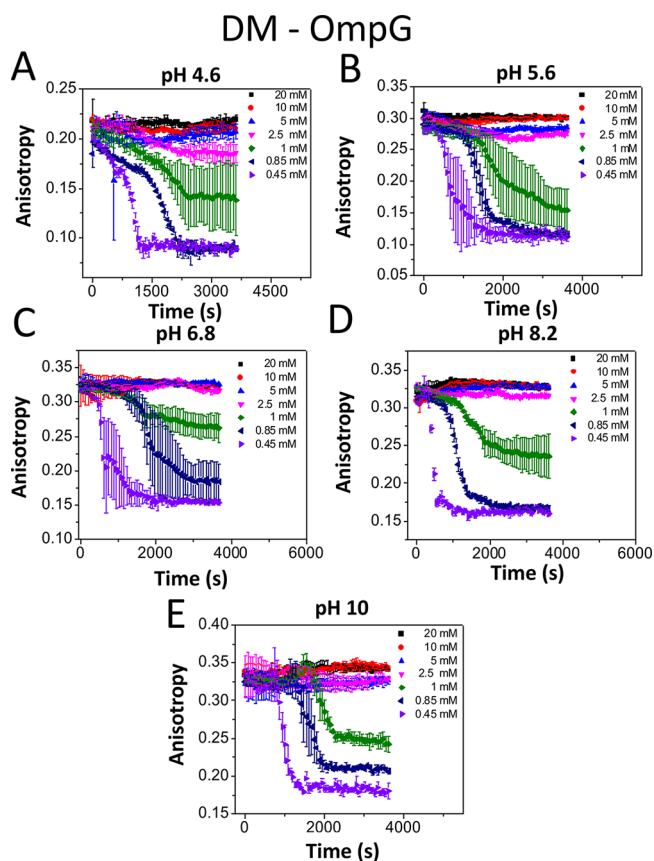


Figure 3. Time-dependent anisotropy showing the DM desolvation of OmpG at various pH values. The starting DM concentration was 20 mM. (A) pH 4.6; (B) pH 5.6; (C) pH 6.8; (D) pH 8.2; (E) pH 10.0. The FP measurements were carried out using a solution that contained 200 mM NaCl at room temperature. The buffer was either 50 mM HEPES (pH 6.8 and 8.2), 50 mM NaOAc (pH 4.6 and 5.6), or 50 mM sodium borate (pH 10.0). All data were derived as averages \pm SD of at least three independent data acquisitions.

a result in the desorption of detergent monomers from proteomicelles. Therefore, for these conditions the FP anisotropy varied between r_{\max} which corresponded to slowly tumbling proteomicelles, and r_{\min} , which was reached under detergent-desolvated conditions (Supporting Information, Figures S4–S21).

The linear and exponential phases of the time-dependent FP anisotropy decrease were employed to determine the apparent zero-order and first-order rate constants of the predesolvation and desolvation processes (Methods), respectively. Usually, the observed predesolvation rate constants ($k_{\text{obs}}^{\text{pre}}$; Supporting Information, Tables S1–S8) and desolvation rate constants ($k_{\text{obs}}^{\text{des}}$; Supporting Information, Tables S9–S16) increased by reducing the detergent concentration within the sample well. By changing the pH, the overall protein charge of a membrane protein is altered. Therefore, we first explored this effect using steady-state FP anisotropy measurements under detergent desolvation conditions. At pH 4.6, the $k_{\text{obs}}^{\text{pre}}$ values for the DM-OmpG proteomicelles acquired at DM concentrations of 1, 0.85, and 0.45 mM were $(1.9 \pm 0.1) \times 10^{-5}$, $(2.0 \pm 0.1) \times 10^{-5}$, and $(5.2 \pm 0.4) \times 10^{-5} \text{ s}^{-1}$, respectively (Figure 3; Supporting Information, Table S1). On the other hand, the corresponding $k_{\text{obs}}^{\text{des}}$ values for similar experimental conditions were $(2.6 \pm 0.3) \times 10^{-3}$, $(3.0 \pm 0.3) \times 10^{-3}$, and $(4.5 \pm 0.5) \times 10^{-3} \text{ s}^{-1}$, respectively (Supporting Information, Table S9). At a

slightly acidic pH of 6.8, the $k_{\text{obs}}^{\text{pre}}$ values were $(0.9 \pm 0.1) \times 10^{-5}$, $(2.1 \pm 0.1) \times 10^{-5}$, and $(4.2 \pm 0.7) \times 10^{-5} \text{ s}^{-1}$, respectively. Under identical experimental conditions, the corresponding $k_{\text{obs}}^{\text{des}}$ values were lower than those noted at pH 4.6, as follows: $(1.3 \pm 0.1) \times 10^{-3}$, $(2.0 \pm 0.1) \times 10^{-3}$, and $(2.4 \pm 0.2) \times 10^{-3} \text{ s}^{-1}$, respectively. On the contrary, higher $k_{\text{obs}}^{\text{des}}$ values were recorded at pH 10: $(2.4 \pm 0.2) \times 10^{-3}$, $(2.7 \pm 0.2) \times 10^{-3}$, and $(5.1 \pm 0.2) \times 10^{-3} \text{ s}^{-1}$, respectively. This nonmonotonic pH-dependence of the $k_{\text{obs}}^{\text{des}}$ values suggests compensatory effects of the numerous heterogeneously distributed electrostatic interactions at the PDC interface. $k_{\text{obs}}^{\text{pre}}$ was less sensitive than $k_{\text{obs}}^{\text{des}}$ upon pH changes. This is an intuitive finding, because it is conceivable that during the predesolvation phase only a limited number of nonionic detergent monomers detach from the proteomicelles.

On the other hand, an atypical desolvation pattern was noted with CYMAL-4-OmpG proteomicelles at pH 4.6 and at 1 and 2 mM CYMAL-4 (Figure 4). For example, the FP

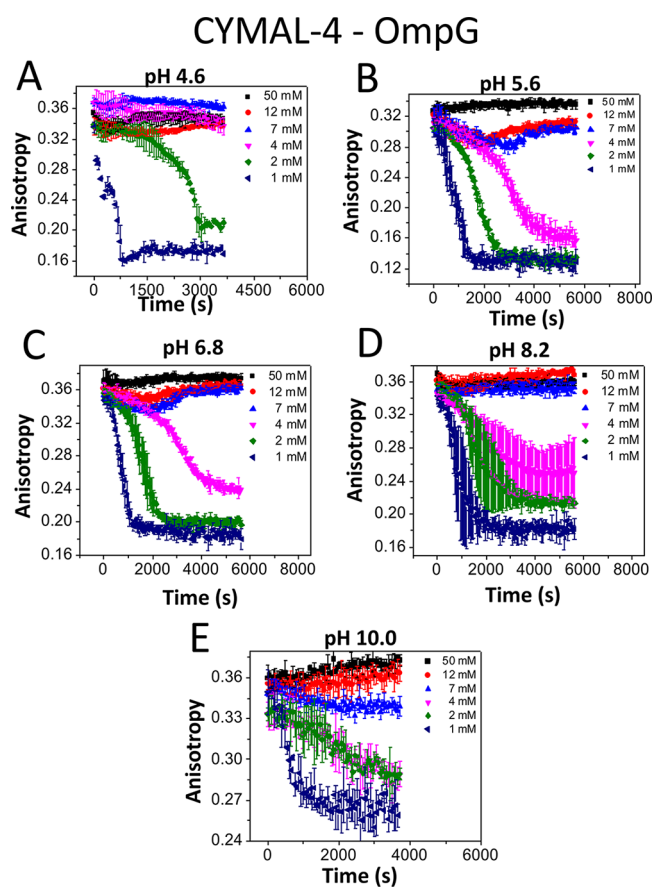


Figure 4. Time-dependent FP anisotropy showing the CYMAL-4 desolvation of OmpG at various pH values. The starting CYMAL-4 concentration was 50 mM. (A) pH 4.6; (B) pH 5.6; (C) pH 6.8; (D) pH 8.2; (E) pH 10.0. The other experimental conditions were the same as those stated in the caption of Figure 3.

anisotropy traces acquired at 1 mM showed a fast desolvation phase, whereas those recorded at 2 mM exhibited a long predesolvation phase. Interestingly, at a CYMAL-4 concentration of 4 mM or greater than this value,²¹ no significant time-dependent FP anisotropy change was noted. At an acidic pH of 5.6, the $k_{\text{obs}}^{\text{pre}}$ values for the CYMAL-4-OmpG proteomicelles at CYMAL-4 concentrations of 4, 2, and 1 mM were $(2.0 \pm 0.1) \times 10^{-5}$, $(3.4 \pm 0.2) \times 10^{-5}$, and $(5.8 \pm$

$0.3) \times 10^{-5} \text{ s}^{-1}$, respectively (Supporting Information, Table S5). The corresponding $k_{\text{obs}}^{\text{des}}$ values for identical conditions were $(1.1 \pm 0.1) \times 10^{-3}$, $(1.7 \pm 0.1) \times 10^{-3}$, and $(2.0 \pm 0.1) \times 10^{-3} \text{ s}^{-1}$, respectively (Supporting Information, Table S13). Under a mildly acidic pH of 6.8, the $k_{\text{obs}}^{\text{pre}}$ values for the CYMAL-4-OmpG proteomicelles at CYMAL-4 concentrations of 4, 2, and 1 mM were $(1.7 \pm 0.1) \times 10^{-5}$, $(2.7 \pm 0.1) \times 10^{-5}$, and $(3.0 \pm 0.6) \times 10^{-5} \text{ s}^{-1}$, respectively. The corresponding $k_{\text{obs}}^{\text{des}}$ values under similar conditions were close to those noted at pH 5.6, as follows: $(1.0 \pm 0.1) \times 10^{-3}$, $(2.0 \pm 0.1) \times 10^{-3}$, and $(2.4 \pm 0.1) \times 10^{-3} \text{ s}^{-1}$, respectively. When these experiments were conducted at pH 10.0, a significant increase in the signal noise was recorded (Figure 4), impeding an accurate determination of the observed rate constants of predesolvation and desolvation.

Apparent First-Order Rate Constants of Detergent Desolvation of the Proteomicelles Depend on the Protein Charge. In the prior results section, we demonstrate that even if the detergent monomers are nonionic the interfacial PDC interactions might be affected by pH. Here, we asked whether these interactions with neutral detergents depend on the overall protein charge. The test case was conducted for radically altered FhuA $\Delta\text{C}/\Delta\text{SL}_{25\text{N}}$ and FhuA $\Delta\text{C}/\Delta\text{SL}_{30\text{N}}$, two homologous FhuA variants whose 25 and 30 negative charges were neutralized with respect to FhuA $\Delta\text{C}/\Delta\text{SL}$ protein. The presence of slow predesolvation and fast desolvation phases were also noted for these proteins that encompassed radical alterations in the overall protein charge (Figures 5–7). At 1 mM DM and pH 5.6, we acquired desolvation rate constants of $(1.6 \pm 0.1) \times 10^{-3}$, $(3.4 \pm 0.2) \times 10^{-3}$, and $(1.1 \pm 0.1) \times 10^{-3} \text{ s}^{-1}$ for FhuA $\Delta\text{C}/\Delta\text{SL}$, FhuA $\Delta\text{C}/\Delta\text{SL}_{25\text{N}}$, and FhuA $\Delta\text{C}/\Delta\text{SL}_{30\text{N}}$, respectively (Figure 8A; Supporting Information, Tables S10–S12). Under similar conditions, but at slightly alkaline pH 8.2, these values were $(1.9 \pm 0.2) \times 10^{-3}$, $(3.4 \pm 0.2) \times 10^{-3}$, and $(2.6 \pm 0.2) \times 10^{-3} \text{ s}^{-1}$, respectively. If the DM concentration was reduced to 0.85 mM, then the $k_{\text{obs}}^{\text{des}}$ values at an acidic pH of 5.6 were $(3.2 \pm 0.1) \times 10^{-3}$, $(3.4 \pm 0.2) \times 10^{-3}$, and $(2.2 \pm 0.1) \times 10^{-3} \text{ s}^{-1}$, respectively (Figure 8B). At the same time, at pH 8.2, a significant reduction in the $k_{\text{obs}}^{\text{des}}$ values was noted for the acidic FhuA derivative, but substantially increased values were determined for the basic FhuA variants. This finding indicates stronger interfacial PDC interactions of the acidic FhuA protein as compared to those corresponding to basic FhuA variants.

The impact of protein electrostatics on adhesive interactions was also noted in the case of CYMAL-4-FhuA proteomicelles. For example, at pH 8.2 the $k_{\text{obs}}^{\text{des}}$ values acquired with the acidic FhuA mutant were significantly smaller than those obtained for the basic FhuA variants (Figure 8C; Supporting Information, Tables S14–S16). Figure 8D illustrates the initial desolvation rates, $R_{\text{in}}^{\text{des}}$ (Methods), which were inferred for various types of proteomicelles at detergent concentrations of 1 mM DM and 4 mM CYMAL-4. These concentrations are about ~55% and ~52% of their corresponding CMC values, respectively. For both cases DM- and CYMAL-4-containing proteomicelles, the initial desolvation rates of the acidic proteins OmpG and FhuA $\Delta\text{C}/\Delta\text{SL}$ were lower than those determined for the basic truncation FhuA mutants (Figure 8D; Supporting Information, Table S17). This outcome suggests stronger adhesive forces of the acidic protein-containing proteomicelles than those interfacial interactions of the basic protein-containing proteomicelles at pH 8.2.

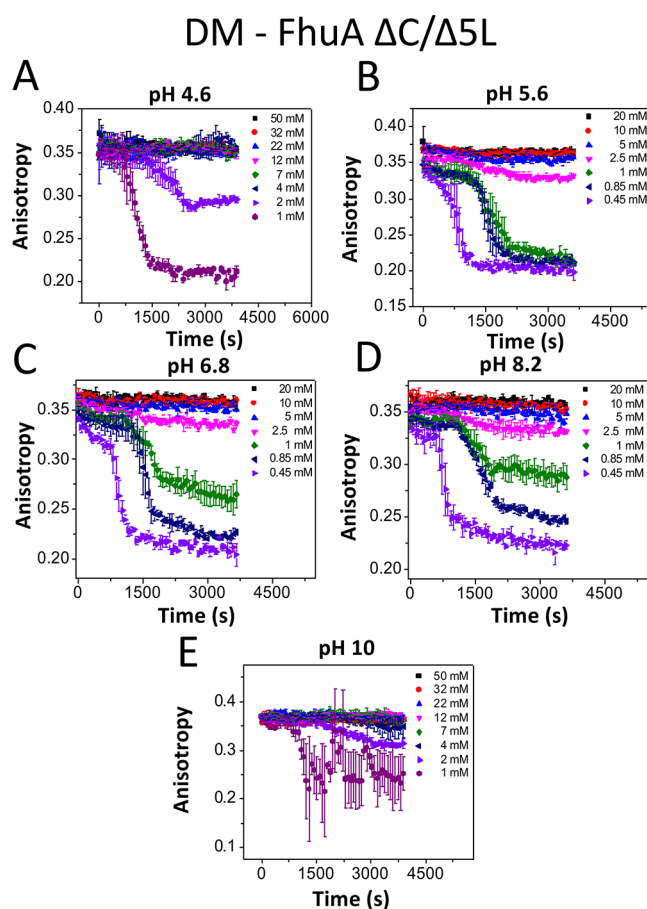


Figure 5. Time-dependent FP anisotropy showing the DM desolvation of FhuA $\Delta\text{C}/\Delta\text{SL}$ at various pH values. (A) pH 4.6; (B) pH 5.6; (C) pH 6.8; (D) pH 8.2; (E) pH 10.0. The other experimental conditions were the same as those stated in the caption of Figure 3.

Kinetics but Not Energetics of the Adhesive PDC Interactions Depend on the Protein Charge. In most cases examined in this study, the $k_{\text{obs}}^{\text{des}}$ values scaled with the detergent concentration in a linear fashion (Supporting Information, Figures S22–S29). Therefore, we formulated a simple kinetic model of proteomicelles, which includes the bimolecular association of a membrane protein with a detergent micelle and unimolecular dissociation of a membrane protein from a micelle (Supporting Information).⁴² The two processes are quantitatively assessed by the apparent model-dependent rate constants of association, k_{on} , and dissociation, k_{off} . These data, which were determined for the four proteins, two maltoside-containing detergents, and three pH values, are illustrated in Figure 9A,B, respectively.

An immediate observation is that the k_{on} values obtained for DM are from several fold to about 1 order of magnitude greater than those determinations acquired for CYMAL-4 (Figure 9A; Supporting Information, Tables S18–S19). For example, these k_{on} values inferred for the most basic protein, FhuA $\Delta\text{C}/\Delta\text{SL}_{30\text{N}}$, and DM-containing proteomicelles were 48 ± 11 , 22 ± 3 , and $63 \pm 14 \text{ M}^{-1} \text{ s}^{-1}$ at pH values of 5.6, 6.8, and 8.2, respectively. Under similar experimental conditions, the k_{on} values for CYMAL-4-containing proteomicelles were 4 ± 1 , 6 ± 1 , and $5 \pm 2 \text{ M}^{-1} \text{ s}^{-1}$, respectively. The fact of the k_{on} values obtained for DM-containing proteomicelles are substantially greater than those inferred for CYMAL-4-containing proteomicelles is in accord with a longer alkyl

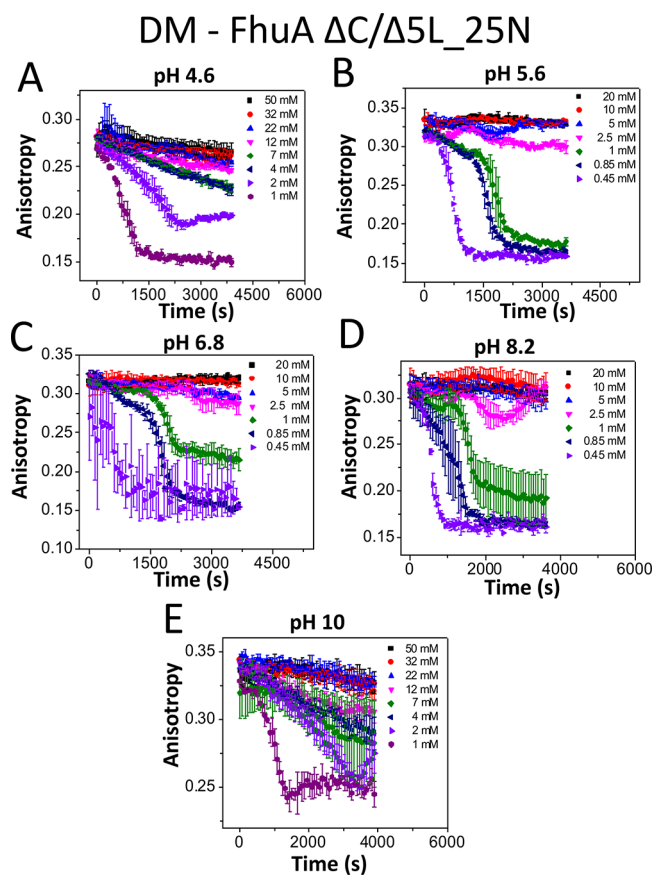


Figure 6. Time-dependent FP anisotropy showing the DM desolvation of FhuA $\Delta C/\Delta 5L_{25N}$ at various pH values. (A) pH 4.6; (B) pH 5.6; (C) pH 6.8; (D) pH 8.2; (E) pH 10.0. The other experimental conditions were the same as those stated in the caption of Figure 3.

chain of DM. The dissociation rate constants, k_{off} , of the DM-containing proteomicelles were also greater than those inferred for the CYMAL-4-containing proteomicelles (Figure 9B). Therefore, the alteration in the hydrophobic interactions at the PDC interface through the length of the alkyl chain has a significant effect on the association rate constants. We were able to calculate the apparent equilibrium dissociation constants of the PDC using the model-dependent k_{on} and k_{off} values (e.g., $K_d = k_{\text{off}}/k_{\text{on}}$). These determinations neglected the contributions of the predesolvation phases (Figure 9C,D). Remarkably, the model-dependent apparent K_d values for DM-containing proteomicelles were comparable with the CMC^{DM} (~ 1.8 mM; Supporting Information, Table S18),^{35,36} suggesting that the adhesion forces between the membrane proteins and DM detergent monomers are well balanced by the cohesive forces among the detergent monomers. Finally, these equilibrium constants were neither dependent on the overall protein charge nor sensitive to alterations in pH, contrasting the outcomes pertaining to observed desolvation constants as well as the rate constants of association and dissociation (Figure 9C,D).

DISCUSSION

In this paper, we show a semiquantitative approach for the determination of model-dependent association and dissociation rate constants of proteomicelles. To the best of our knowledge, this is the first kinetic method of proteomicelles

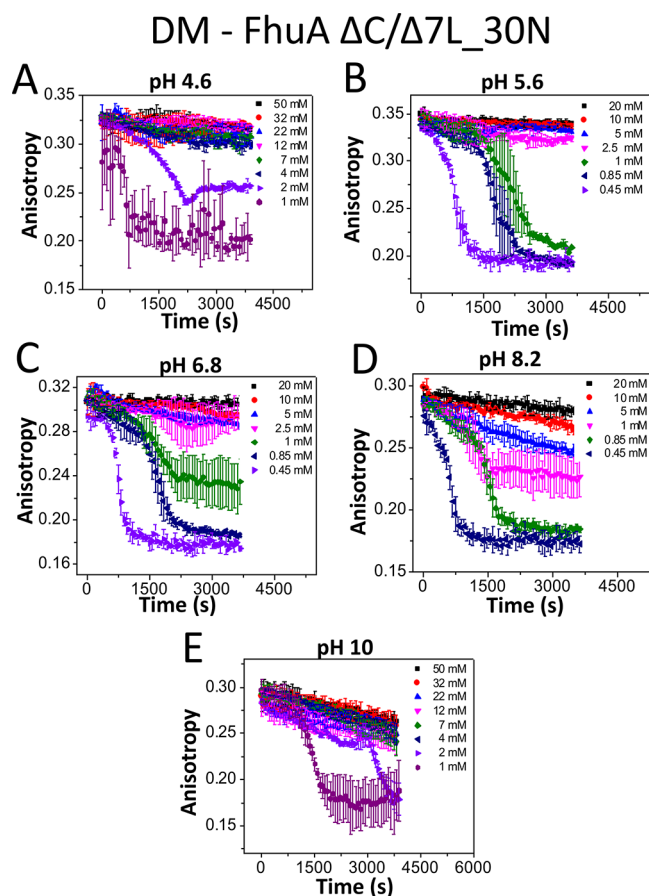


Figure 7. Time-dependent FP anisotropy showing the DM desolvation of FhuA $\Delta C/\Delta 7L_{N30}$ at various pH values. (A) pH 4.6; (B) pH 5.6; (C) pH 6.8; (D) pH 8.2; (E) pH 10.0. The other experimental conditions were the same as those stated in the caption of Figure 3.

that has potential for high-throughput screening,^{19,20} because of its amenability to a 1536-well, plate-reader format. The central player of this approach is a bright,^{39,44} optically stable,^{39,44} and pH insensitive⁴⁵ Texas Red fluorophore. In addition, the photophysics of Texas Red is not sensitive to its environmental changes,⁴⁶ permitting these extensive measurements in a fairly broad range of physical and chemical circumstances. Here, Texas Red was covalently attached either on a flexible loop (e.g., OmpG) or on a β turn (e.g., FhuA derivative) using maleimide chemistry. Because the fluorophore was not located within the core of the folded β -barrel protein, but at its periphery, the recorded FP anisotropy is not directly related to protein folding, contrasting an intrinsic, internal tryptophan probe.¹³ A sharp decrease in the FP anisotropy is most likely directly determined by the reduction in the hydrodynamic radius of the proteomicelle, R_h , resulting from detergent desorption at the protein surface. Therefore, we think that FP anisotropy curves are not expectedly sensitive to changes in the site of fluorescent labeling on the protein surface.

Recently, we have used this approach for screening detergents of varying physicochemical properties in order to select those that exhibit satisfactory solubilizing features.²¹ The value of the steady-state FP anisotropy followed a two-state transition when the protein sample was brought from a detergent concentration greater than the CMC to a detergent

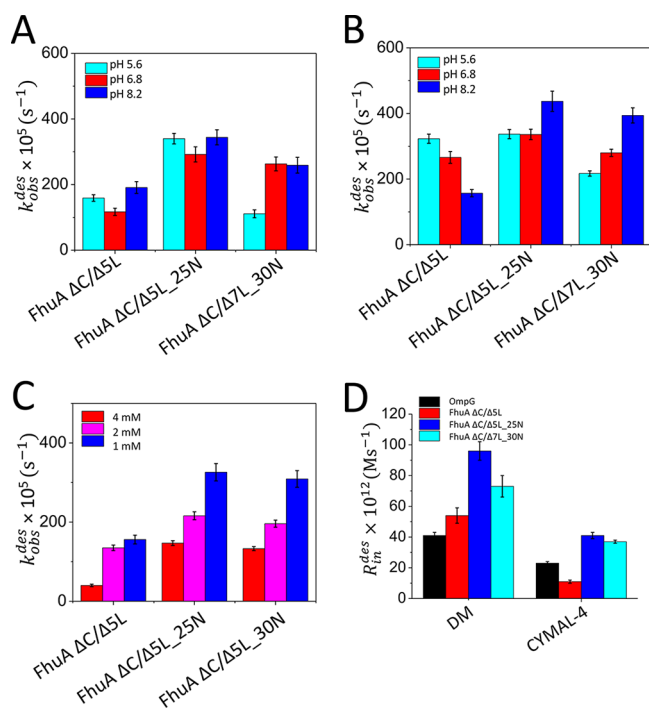


Figure 8. Dependence of the observed desolvation rate constants, k_{obs}^{des} , on the protein charge. (A) The values were determined for the DM desolvation of FhuA $\Delta C/\Delta 5L$, FhuA $\Delta C/\Delta 5L_{25N}$, and FhuA $\Delta C/\Delta 7L_{30N}$ at 1 mM DM. (B) The values were determined for the DM desolvation of FhuA $\Delta C/\Delta 5L$, FhuA $\Delta C/\Delta 5L_{25N}$, and FhuA $\Delta C/\Delta 7L_{30N}$ at 0.85 mM DM. (C) The values were determined for the CYMAL-4 desolvation of FhuA $\Delta C/\Delta 5L$, FhuA $\Delta C/\Delta 5L_{25N}$, and FhuA $\Delta C/\Delta 7L_{30N}$ at pH 8.2. Different vertical columns show data acquired at various CYMAL-4 concentrations. (D) Illustration of the initial desolvation rates, R_{in}^{des} , which were determined for proteins of varying overall charge at pH 8.2. The final detergent concentrations for DM and CYMAL-4 were 1 and 4 mM, respectively. The other experimental conditions were the same as those stated in the caption of Figure 3.

concentration below the CMC. The isothermal detergent desorption curves were used to infer the equilibrium dissociation constants of the proteomicelles containing α -helical membrane proteins.³⁵ The process of detergent desorption showed the existence of slow predesolvation and fast desolvation phases for detergents with excellent solubilizing characteristics.³³ The kinetic details of the interfacial PDC interactions represent a foundation for developing novel protocols employed in the functional reconstitution of membrane proteins. Previously, isothermal titration calorimetry (ITC)⁴⁷ has been successfully employed to unravel equilibrium phase diagrams of complex ternary mixtures of lipid-detergent-protein systems.^{11,48} This information has practical implications for the protein reconstitution into lipid vesicles.

Our FP anisotropy approach is also facilitated by the fact that the steady-state FP anisotropy is insensitive to changes in protein concentration.⁴⁹ Accordingly, a gradual decrease in the effective detergent-solubilized protein concentration, which potentially results from unproductive aggregation,^{10,12} does not impair the optical signal-to-noise ratio. Indeed, the truncation FhuA variants are highly prone to aggregation as a result of detergent depletion within the sample well at concentrations well below the CMC. Despite these environmentally harsh conditions for these β -barrel membrane proteins, we were still

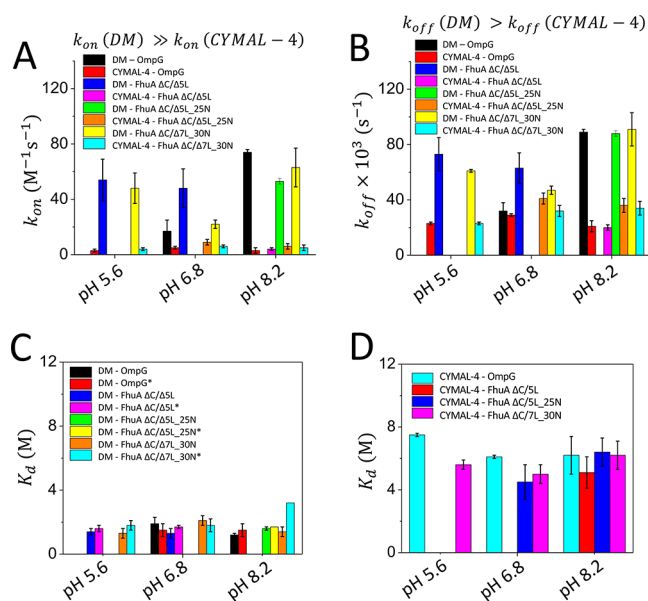


Figure 9. Apparent rate constants of the interfacial PDC interactions of proteomicelles. (A) The association rate constants of DM-containing proteomicelles are much greater than those of CYMAL-4-containing proteomicelles. (B) The dissociation rate constants of DM-containing proteomicelles are greater than those of CYMAL-4-containing proteomicelles. (C) The model-dependent (this work) and model-free³⁵ equilibrium dissociation constants, K_d , of the DM-containing proteomicelles. (D) The model-dependent apparent dissociation constants, K_d , of the CYMAL-4-containing proteomicelles. The other experimental conditions were the same as those stated in the caption of Figure 3.

able to measure time-dependent changes in the FP anisotropy that reflect the decrease of the proteomicelle size in a reproducible fashion. Gradual protein aggregation might have various effects on the FP readout, including quenching. According to Perrin's equation,²⁰ r_0/r is an additive function of $6D_r/\tau_F$ where r_0 , r , D_r and τ_F denote the fundamental maximum FP anisotropy, recorded steady-state FP anisotropy, rotational diffusion coefficient of the proteomicelle, and fluorescence lifetime of the fluorophore, respectively. Therefore, quenching increases the FP anisotropy. Second, protein aggregation, even without quenching, decreases the tumbling rate of the detergent-desolvated proteins. Third, it is conceivable that a residual amount of bound detergent monomers still exists under detergent depletion conditions. These effects likely increase the r_{min} values depending on their relative impact on the raw FP signal at detergent concentrations much lower than the CMC. In accord with these expectations, we often observed elevated r_{min} states in these FP anisotropy measurements. The truncation FhuA variants exhibit an r_{min} of ~ 0.16 under fully denaturing conditions in the presence of chaotropic agents,²¹ but time-dependent FP anisotropy measurements during detergent desolvation phase at times showed the r_{min} values even greater than 0.2.

On the other hand, at detergent concentrations much greater than the CMC, we recorded high FP anisotropy values with r_{max} of ~ 0.3 or even greater, approaching the fundamental maximum FP anisotropy, r_0 ($r_0 = 0.4$).⁵⁰ This reason is primarily determined by probing relatively slow rotational diffusion mobilities of the membrane proteins. Under these conditions, the diffusional correlation times are slightly greater than the fluorescence lifetime of Texas Red ($\tau_F = 4.2$ ns).⁴⁴

High anisotropy data points indicate that the majority of the emitted photons maintain their original polarization. The high FP anisotropy is related not only to the size of the membrane protein but also to the overall size of micelles, so that these values are expected under detergent-mediated refolding conditions.

Different groups routinely recorded steady-state FP anisotropy values of ~ 0.3 under equilibrium conditions.^{44,49,51,52} For example, Qiao and co-workers (2011) found anisotropy changes between 0.1 and 0.3 when Texas Red was attached to short peptides forming complexes with antibodies.⁵³ Again, such a high FP anisotropy value of ~ 0.3 is expected under conditions in which the tumbling rate of the peptide–protein complex is drastically slowed down. Here, we provide compelling evidence for the high sensitivity and specificity of our method, which in many examples feature FP anisotropy changes of ~ 0.15 , namely $\sim 38\%$ out of the maximum anisotropy range. Interestingly, at final detergent concentrations much greater than the CMC, the steady-state FP anisotropy remains fairly unchanged at a value r_{\max} , suggesting that the proteomicelles reach the lowest rotational mobilities under this experimental circumstance. This situation corresponds to the highest hydrodynamic radius of proteomicelles. Such an outcome is somewhat counterintuitive, because of the gradually enhanced solution viscosity at increased detergent concentrations. However, our finding is in good accord with prior NMR studies performed by Stanczak and co-workers,⁵⁴ who also discovered that the hydrodynamic radius of the PDC containing *n*-decylphosphocholine (Fos-10) and outer membrane protein X (OmpX) is not affected by greatly increased Fos-10 concentrations above the CMC.

The observed predesolvation and desolvation rate constants depend on the alkyl chain of the detergent monomers, charge of the membrane protein, and pH of the interfacial PDC space. These variables modulate the adhesion forces of the proteomicelles between detergent monomers and membrane proteins. Notably, the observed desolvation rate constants, $k_{\text{obs}}^{\text{des}}$, are generally greater for the basic homologous FhuA variants than those acquired for the acidic proteins OmpG and FhuA $\Delta C/\Delta SL$. A deviation from this trend occurred for DM-containing proteomicelles at pH 5.6 and 0.85 mM DM. It should be noted that changing the pH would also change the overall protein charge, explaining at least in part the nonmonotonic nature of the pH dependence of $k_{\text{obs}}^{\text{des}}$. Furthermore, the initial desolvation rates, $R_{\text{in}}^{\text{des}}$, of the DM- and CYMAL-4-containing proteomicelles were also greater for the basic proteins than those obtained for the acidic β -barrels. This finding suggests that the adhesive interactions at the PDC interface⁵⁵ are generally stronger for the acidic proteins than those for the basic ones. These results agree well with prior studies that indicated satisfactory solubilization traits of nonionic *n*-octyl- β -D-glucoside (OG) for acidic but not basic β -barrels.²¹

CONCLUSIONS

In summary, we show time-dependent kinetic determinations of proteomicelles containing β -barrel membrane proteins of varying isoelectric point. The model-dependent apparent K_d values are fairly independent of pH and protein charge, but they are comparable with or slightly lower than the CMC. Because the affinity constants of the PDC interactions are closely similar to the corresponding CMC, these inspected β -barrel membrane proteins are poor nucleators of the

proteomicellization process. Therefore, the detergent monomers have little discrimination in associating either with the proteins or with themselves. The high equilibrium dissociation constants, in the millimolar range, are primarily caused by low association rate constants of the proteomicelles. Small k_{on} values, lower than $10^2 \text{ M}^{-1} \text{ s}^{-1}$, provide a quantitative confirmation of fairly low diffusion coefficients of hydrophobic molecules, either detergent monomers or membrane proteins, in aqueous phase. Further adaptations of this approach will likely impact accelerated discoveries in the synthetic chemistry of nonconventional detergents⁵⁶ as well as in the structural, physical, and chemical biology of membrane proteins.

ASSOCIATED CONTENT

Supporting Information

These materials are available free of charge via the Internet at The Supporting Information is available free of charge on the ACS Publications website at DOI: 10.1021/acs.jpcc.8b07889.

- Time-dependent FP anisotropy changes of membrane proteins of varying isoelectric point (pI) at detergent incubations above and below the CMC, and in buffers of varying pH;
- curve fits of the predesolvation and desolvation phases at detergent concentrations below the CMC and in buffers of varying pH;
- determination of the predesolvation rates of protein nanopores of varying pI, at detergent concentrations below the CMC, and in buffers of varying pH;
- determination of the desolvation rate and time constants of protein nanopores of varying pI, and at detergent concentrations below the CMC, and in buffers of varying pH;
- initial desolvation rates determined for acidic and basic β -barrel membrane proteins;
- calculation of the association (k_{on}) and dissociation (k_{off}) rate constants using detergent desolvation curves;
- scaling of the observed desolvation rates of the protein nanopores with the detergent concentrations at values below the CMC;
- kinetic rate constants of association and dissociation of proteomicelles using time-dependent FP anisotropy changes (PDF)

AUTHOR INFORMATION

Corresponding Author

*Phone: 315-443-8078. Fax: 315-443-9103. E-mail: lmovilea@syr.edu.

ORCID

Min Chen: 0000-0002-7572-0761

Liviu Movileanu: 0000-0002-2525-3341

Author Contributions

[†]A.J.W. and J.F.G. contributed equally to this work.

Notes

The authors declare no competing financial interest.

ACKNOWLEDGMENTS

We thank Yi-Ching Hsueh, Adam Blanden, and Bach Pham for their assistance during the very early stage of these studies. The authors are also grateful to Motahareh Ghahari Larimi and Lauren Mayse for their comments and stimulating discussions. This research was supported by the U.S. National Institutes of Health Grants GM115442 (to M.C.), GM088403 (to L.M.), and GM129429 (to L.M.).

REFERENCES

- (1) Reading, E.; Liko, I.; Allison, T. M.; Benesch, J. L.; Laganowsky, A.; Robinson, C. V. The role of the detergent micelle in preserving the structure of membrane proteins in the gas phase. *Angew. Chem., Int. Ed.* **2015**, *54*, 4577–81.
- (2) Kleinschmidt, J. H. Folding of beta-barrel membrane proteins in lipid bilayers - Unassisted and assisted folding and insertion. *Biochim. Biophys. Acta, Biomembr.* **2015**, *1848*, 1927–43.
- (3) Nadeau, V. G.; Rath, A.; Deber, C. M. Sequence hydrophathy dominates membrane protein response to detergent solubilization. *Biochemistry* **2012**, *51*, 6228–37.
- (4) Pollock, N. L.; Satriano, L.; Zegarra-Moran, O.; Ford, R. C.; Moran, O. Structure of wild type and mutant F508del CFTR: A small-angle X-ray scattering study of the protein-detergent complexes. *J. Struct. Biol.* **2016**, *194*, 102–11.
- (5) Stangl, M.; Veerappan, A.; Kroeger, A.; Vogel, P.; Schneider, D. Detergent properties influence the stability of the glycophorin A transmembrane helix dimer in lysophosphatidylcholine micelles. *Biophys. J.* **2012**, *103*, 2455–64.
- (6) Yang, Z.; Wang, C.; Zhou, Q.; An, J.; Hildebrandt, E.; Aleksandrov, L. A.; Kappes, J. C.; DeLucas, L. J.; Riordan, J. R.; Urbatsch, I. L.; et al. Membrane protein stability can be compromised by detergent interactions with the extramembranous soluble domains. *Protein Sci.* **2014**, *23*, 769–89.
- (7) Rath, A.; Glibowicka, M.; Nadeau, V. G.; Chen, G.; Deber, C. M. Detergent binding explains anomalous SDS-PAGE migration of membrane proteins. *Proc. Natl. Acad. Sci. U. S. A.* **2009**, *106*, 1760–5.
- (8) Frey, L.; Lakomek, N. A.; Riek, R.; Bibow, S. Micelles, bicelles, and nanodiscs: comparing the impact of membrane mimetics on membrane protein backbone dynamics. *Angew. Chem., Int. Ed.* **2017**, *56*, 380–383.
- (9) Crichton, P. G.; Harding, M.; Ruprecht, J. J.; Lee, Y.; Kunji, E. R. Lipid, detergent, and Coomassie Blue G-250 affect the migration of small membrane proteins in blue native gels: mitochondrial carriers migrate as monomers not dimers. *J. Biol. Chem.* **2013**, *288*, 22163–73.
- (10) Neale, C.; Ghanei, H.; Holyoake, J.; Bishop, R. E.; Prive, G. G.; Pomes, R. Detergent-mediated protein aggregation. *Chem. Phys. Lipids* **2013**, *169*, 72–84.
- (11) Jahnke, N.; Krylova, O. O.; Hoomann, T.; Vargas, C.; Fiedler, S.; Pohl, P.; Keller, S. Real-time monitoring of membrane-protein reconstitution by isothermal titration calorimetry. *Anal. Chem.* **2014**, *86*, 920–927.
- (12) Khelashvili, G.; LeVine, M. V.; Shi, L.; Quick, M.; Javitch, J. A.; Weinstein, H. The membrane protein LeuT in micellar systems: aggregation dynamics and detergent binding to the S2 site. *J. Am. Chem. Soc.* **2013**, *135*, 14266–75.
- (13) Horne, J. E.; Radford, S. E. A growing toolbox of techniques for studying beta-barrel outer membrane protein folding and biogenesis. *Biochem. Soc. Trans.* **2016**, *44*, 802–9.
- (14) Sadaf, A.; Cho, K. H.; Byrne, B.; Chae, P. S. Amphipathic agents for membrane protein study. *Methods Enzymol.* **2015**, *557*, 57–94.
- (15) Ehsan, M.; Du, Y.; Scull, N. J.; Tikhonova, E.; Tarrasch, J.; Mortensen, J. S.; Loland, C. J.; Skiniotis, G.; Guan, L.; Byrne, B.; et al. Highly branched pentasaccharide-bearing amphiphiles for membrane protein studies. *J. Am. Chem. Soc.* **2016**, *138*, 3789–96.
- (16) Das, M.; Du, Y.; Ribeiro, O.; Hariharan, P.; Mortensen, J. S.; Patra, D.; Skiniotis, G.; Loland, C. J.; Guan, L.; Kobilka, B. K.; et al. Conformationally preorganized diastereomeric norbornane-based maltosides for membrane protein study: implications of detergent kink for micellar properties. *J. Am. Chem. Soc.* **2017**, *139*, 3072–3081.
- (17) Yengo, C. M.; Berger, C. L. Fluorescence anisotropy and resonance energy transfer: powerful tools for measuring real time protein dynamics in a physiological environment. *Curr. Opin. Pharmacol.* **2010**, *10*, 731–7.
- (18) Rossi, A. M.; Taylor, C. W. Analysis of protein-ligand interactions by fluorescence polarization. *Nat. Protoc.* **2011**, *6*, 365–87.
- (19) Lea, W. A.; Simeonov, A. Fluorescence polarization assays in small molecule screening. *Expert Opin. Drug Discovery* **2011**, *6*, 17–32.
- (20) Zhang, H.; Wu, Q.; Berezin, M. Y. Fluorescence anisotropy (polarization): from drug screening to precision medicine. *Expert Opin. Drug Discovery* **2015**, *10*, 1145–61.
- (21) Wolfe, A. J.; Hsueh, Y. C.; Blanden, A. R.; Mohammad, M. M.; Pham, B.; Thakur, A. K.; Loh, S. N.; Chen, M.; Movileanu, L. Interrogating detergent desolvation of nanopore-forming proteins by fluorescence polarization spectroscopy. *Anal. Chem.* **2017**, *89*, 8013–8020.
- (22) Ayub, M.; Bayley, H. Engineered transmembrane pores. *Curr. Opin. Chem. Biol.* **2016**, *34*, 117–126.
- (23) Slusky, J. S. Outer membrane protein design. *Curr. Opin. Struct. Biol.* **2017**, *45*, 45–52.
- (24) Yildiz, O.; Vinothkumar, K. R.; Goswami, P.; Kuhlbrandt, W. Structure of the monomeric outer-membrane porin OmpG in the open and closed conformation. *EMBO J.* **2006**, *25*, 3702–3713.
- (25) Locher, K. P.; Rees, B.; Koebnik, R.; Mitschler, A.; Moulinier, L.; Rosenbusch, J. P.; Moras, D. Transmembrane signaling across the ligand-gated FhuA receptor: crystal structures of free and ferrichrome-bound states reveal allosteric changes. *Cell* **1998**, *95*, 771–778.
- (26) Liu, Z.; Ghai, I.; Winterhalter, M.; Schwaneberg, U. Engineering Enhanced Pore Sizes Using FhuA Delta1–160 from *E. coli* Outer Membrane as Template. *ACS Sens* **2017**, *2*, 1619–1626.
- (27) Mohammad, M. M.; Howard, K. R.; Movileanu, L. Redesign of a plugged beta-barrel membrane protein. *J. Biol. Chem.* **2011**, *286*, 8000–8013.
- (28) Chen, M.; Khalid, S.; Sansom, M. S.; Bayley, H. Outer membrane protein G: engineering a quiet pore for biosensing. *Proc. Natl. Acad. Sci. U. S. A.* **2008**, *105*, 6272–6277.
- (29) Thakur, A. K.; Larimi, M. G.; Gooden, K.; Movileanu, L. Aberrantly large single-channel conductance of polyhistidine arm-containing protein nanopores. *Biochemistry* **2017**, *56*, 4895–4905.
- (30) Mohammad, M. M.; Iyer, R.; Howard, K. R.; McPike, M. P.; Borer, P. N.; Movileanu, L. Engineering a rigid protein tunnel for biomolecular detection. *J. Am. Chem. Soc.* **2012**, *134*, 9521–9531.
- (31) Wolfe, A. J.; Mohammad, M. M.; Thakur, A. K.; Movileanu, L. Global redesign of a native beta-barrel scaffold. *Biochim. Biophys. Acta, Biomembr.* **2016**, *1858*, 19–29.
- (32) Niedzwiecki, D. J.; Mohammad, M. M.; Movileanu, L. Inspection of the engineered FhuA deltaC/delta4L protein nanopore by polymer exclusion. *Biophys. J.* **2012**, *103*, 2115–2124.
- (33) Wolfe, A. J.; Gugel, J. F.; Chen, M.; Movileanu, L. Detergent Desorption of Membrane Proteins Exhibits Two Kinetic Phases. *J. Phys. Chem. Lett.* **2018**, *9*, 1913–1919.
- (34) Fahie, M.; Chisholm, C.; Chen, M. Resolved single-molecule detection of individual species within a mixture of anti-biotin antibodies using an engineered monomeric nanopore. *ACS Nano* **2015**, *9*, 1089–1098.
- (35) Wolfe, A. J.; Si, W.; Zhang, Z.; Blanden, A. R.; Hsueh, Y. C.; Gugel, J. F.; Pham, B.; Chen, M.; Loh, S. N.; Rozovsky, S.; et al. Quantification of membrane protein-detergent complex interactions. *J. Phys. Chem. B* **2017**, *121*, 10228–10241.
- (36) Linke, D. Detergents: an overview. *Methods Enzymol.* **2009**, *463*, 603–617.
- (37) Titus, J. A.; Haugland, R.; Sharrow, S. O.; Segal, D. M. Texas Red, a hydrophilic, red-emitting fluorophore for use with fluorescein in dual parameter flow microfluorometric and fluorescence microscopic studies. *J. Immunol. Methods* **1982**, *50*, 193–204.
- (38) Jameson, D. M.; Ross, J. A. Fluorescence polarization/anisotropy in diagnostics and imaging. *Chem. Rev.* **2010**, *110*, 2685–708.
- (39) Gradinaru, C. C.; Marushchak, D. O.; Samim, M.; Krull, U. J. Fluorescence anisotropy: from single molecules to live cells. *Analyst* **2010**, *135*, 452–9.
- (40) Splinter, R. H. B. A. *An introduction to biomedical optics*; Taylor & Francis: New York, 2007; p 602.

(41) Movileanu, L.; Cheley, S.; Howorka, S.; Braha, O.; Bayley, H. Location of a constriction in the lumen of a transmembrane pore by targeted covalent attachment of polymer molecules. *J. Gen. Physiol.* **2001**, *117*, 239–251.

(42) Stoddart, L. A.; White, C. W.; Nguyen, K.; Hill, S. J.; Pflieger, K. D. Fluorescence- and bioluminescence-based approaches to study GPCR ligand binding. *Br. J. Pharmacol.* **2016**, *173*, 3028–3037.

(43) Grosse, W.; Psakis, G.; Mertins, B.; Reiss, P.; Windisch, D.; Brademann, F.; Burck, J.; Ulrich, A.; Koert, U.; Essen, L. O. Structure-based engineering of a minimal porin reveals loop-independent channel closure. *Biochemistry* **2014**, *53*, 4826–38.

(44) Lakowicz, J. R. *Principles of fluorescence microscopy*, 2nd ed.; Springer: New York, 2006.

(45) Ji, J.; Rosenzweig, N.; Griffin, C.; Rosenzweig, Z. Synthesis and application of submicrometer fluorescence sensing particles for lysosomal pH measurements in murine macrophages. *Anal. Chem.* **2000**, *72*, 3497–503.

(46) Unruh, J. R.; Gokulrangan, G.; Wilson, G. S.; Johnson, C. K. Fluorescence properties of fluorescein, tetramethylrhodamine and Texas Red linked to a DNA aptamer. *Photochem. Photobiol.* **2005**, *81*, 682–90.

(47) Heerklotz, H. H.; Binder, H.; Epanand, R. M. A "release" protocol for isothermal titration calorimetry. *Biophys. J.* **1999**, *76*, 2606–13.

(48) Heerklotz, H.; Tsamaloukas, A. D.; Keller, S. Monitoring detergent-mediated solubilization and reconstitution of lipid membranes by isothermal titration calorimetry. *Nat. Protoc.* **2009**, *4*, 686–97.

(49) Li, J.; Qiu, X. J. Quantification of membrane protein self-association with a high-throughput compatible fluorescence assay. *Biochemistry* **2017**, *56*, 1951–1954.

(50) Prazeres, T. J. V.; Fedorov, A.; Barbosa, S. P.; Martinho, J. M. G.; Berberan-Santos, M. N. Accurate determination of the limiting anisotropy of rhodamine 101. Implications for its use as a fluorescence polarization standard. *J. Phys. Chem. A* **2008**, *112*, 5034–5039.

(51) Neves, P.; Lopes, S. C.; Sousa, I.; Garcia, S.; Eaton, P.; Gameiro, P. Characterization of membrane protein reconstitution in LUVs of different lipid composition by fluorescence anisotropy. *J. Pharm. Biomed. Anal.* **2009**, *49*, 276–81.

(52) Heidebrecht, T.; Fish, A.; von Castelmur, E.; Johnson, K. A.; Zaccai, G.; Borst, P.; Perrakis, A. Binding of the J-binding protein to DNA containing glucosylated hmU (base J) or 5-hmC: evidence for a rapid conformational change upon DNA binding. *J. Am. Chem. Soc.* **2012**, *134*, 13357–65.

(53) Qiao, Y.; Tang, H.; Munske, G. R.; Dutta, P.; Ivory, C. F.; Dong, W. J. Enhanced fluorescence anisotropy assay for human cardiac troponin I and T detection. *J. Fluoresc.* **2011**, *21*, 2101–10.

(54) Stanczak, P.; Horst, R.; Serrano, P.; Wuthrich, K. NMR characterization of membrane protein-detergent micelle solutions by use of microcoil equipment. *J. Am. Chem. Soc.* **2009**, *131*, 18450–6.

(55) Khao, J.; Arce-Lopera, J.; Sturgis, J. N.; Duneau, J. P. Structure of a protein-detergent complex: the balance between detergent cohesion and binding. *Eur. Biophys. J.* **2011**, *40*, 1143–55.

(56) Yang, Z.; Brouillette, C. G. A guide to differential scanning calorimetry of membrane and soluble proteins in detergents. *Methods Enzymol.* **2016**, *567*, 319–58.

(57) Mohammad, M. M.; Movileanu, L. Impact of distant charge reversals within a robust beta-barrel protein pore. *J. Phys. Chem. B* **2010**, *114*, 8750–8759.